IMPLEMENTING THE STRATEGIC ACTION PROGRAMME FOR THE YELLOW SEA LARGE MARINE ECOSYSTEM: RESTORING ECOSYSTEM GOODS AND SERVICES AND CONSOLIDATION OF A LONG-TERM REGIONAL ENVIRONMENTAL GOVERNANCE FRAMEWORK

(UNDP/GEF YSLME Phase II Project)

Stocktaking report for the relationships between the sea surface temperature changes of YSCWM and structure of plankton communities

Prepared by

Dr. Hongjun Song & Dr. Zhaohui Zhang

First Institute of Oceanography, MNR

2019.10

Contents

1. Background

As the YSLME project defined, the Yellow Sea is the semi-enclosed body of water bounded as follows: to the west by the Chinese mainland south of Penglai and a line from Penglai to Dalian; to the east by the Korean Peninsula and Cheju Island and a line drawn from Jindo Island off the south coast of the Korean mainland to the north coast of Cheju Island; and to the south by a line running from the north bank of the mouth of the Yangtze River (Chang Jiang) to the southwestern coast of Cheju Island.

Yellow Sea Cold Water Mass (YSCWM) is a unique hydrographic phenomenon in the Yellow Sea. This water mass is located in the central trough of the Yellow Sea. In spring increased solar radiation heats the Yellow Sea, but the water in the central trough, which is a remnant of cold, vertically well mixed water in the previous winter, remains cold because of the depth. As temperature gradient around the water becomes greater in spring through summer, the water is distinctively seen as a dome on the trough. The strong temperature gradient prevents the heat transfer from the surrounding so that the water can remain cold until breaking down in early winter (November). This cold water, because it is more noticeable in the temperature field, is called the Yellow Sea Cold Water Mass (YSCWM) in many literatures (*Park et al.*, 2011).

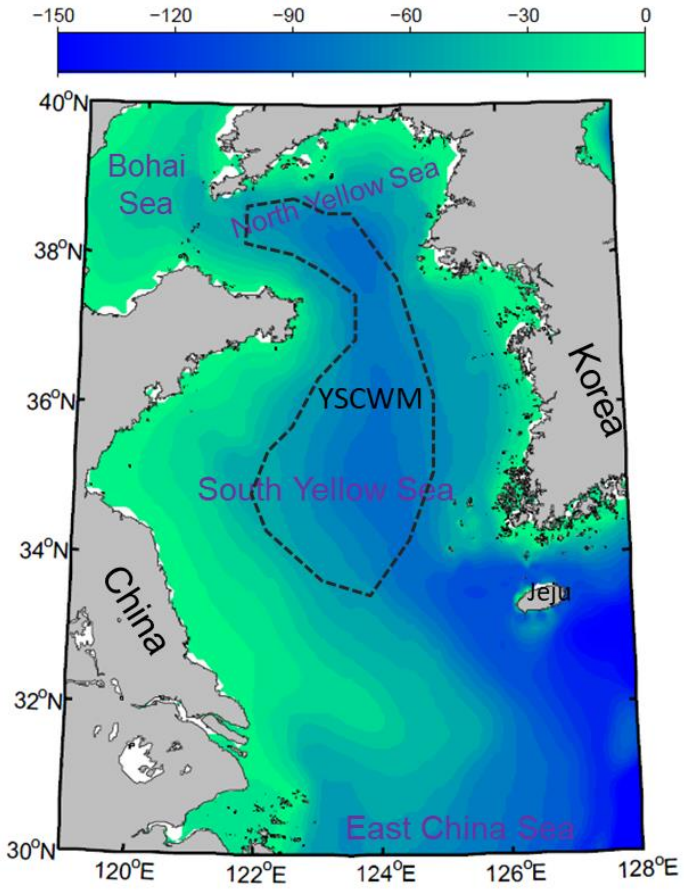

Fig. 1 Geography and location of YSCWM. Area with temperature at 50m colder than 11 ℃ in August were selected as the YSCWM region.

Since YSCWM is the most conservative among water masses in the Yellow Sea, it is likely to contain clearer long-term signals than any other water masses in the YS. The long-term signals are essential to understand climatological evolutions of the YS. The year-to-year variation of YSCWM influences catches and fishing grounds of demersal fishes. YSCWM serves as an oversummering site for many temperate species (*Wang et al., 2003*). The intensity of summer southward/southeastward migration of YSCWM including the cold water over the eastern Yangtze Bank affects the upstream path of the Tsushima Warm Current, and eventually induces

changes in the regional hydrography in the southern Yellow Sea and the northern East China Sea (*Park and Chu, 2006*).

In this report, we first summarize the environmental changes and the spatiotemporal characteristics of plankton communities in the YSCWM region from the existing publications. Then, we try to evaluate the relationships between the environmental changes of YSCWM and structure of plankton communities.

2. Environmental changes in the YSCWM region

2.1 Temperature

Based on a set of seasonally monitored data along a transect (at 36°N) maintained by the State Oceanic Administration of China, an ascending trend was found in sea surface temperature in the Yellow Sea (Fig. 2). The annual mean rates of change were between 0.038 and 0.094 °C. The regional mean of water column average temperature increased 1.7 °C during the observation period. This increase is significant. The warming of seawater in the Yellow Sea during 1976–2000 is consistent with the increase in the mean air temperature observed throughout northern China and the increase in SST found in both the Bohai Sea and the East China Sea (Lin et al, 2005).

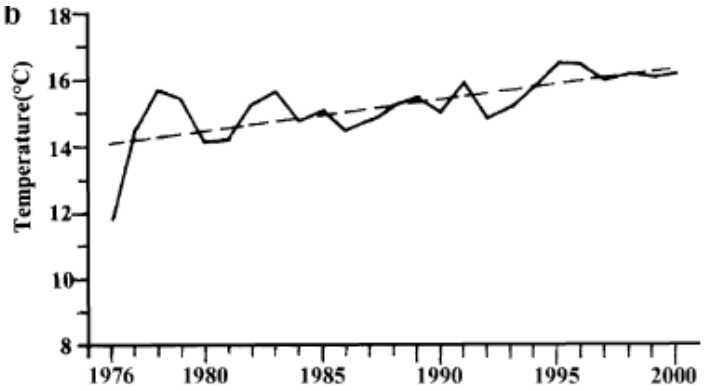

Fig. 2 Sea surface temperature changes in the Yellow Sea (36°N transect data, Lin et al, 2005)

SST anomaly time-series of the KODC dataset at 125°E, 35.9°N and the global dataset at 124°E, 36.0°N were also examined in Park *et al* (2011). The global SST anomaly varies at a smaller extent because of differences in observation methods and preprocesses between the two datasets, whereas the KODC SST anomaly shows larger variability: the KODC SST is ~1.5 °C higher (lower) in August (February and April) than the global SST (Fig. 3a). However, the similarity in the long term variation trend between the two time-series is perceived by the undulating peaks of them. This similarity is more evident in the time series of spatially-averaged non-seasonal SST anomaly (Fig. 3b). Another global dataset, International Comprehensive Ocean–atmosphere Data Set (ICOADS), shows the similar features as well. Since the seasonal cycle was deleted, the range of the variability is almost the same, −1.2 °C to 1.4 °C, among the three time-series. Although the KODC time-series retains more short-term features, the three datasets are consistent in the long-term scales such as interannual to interdecadal scales with the correlation coefficient of 0.8.

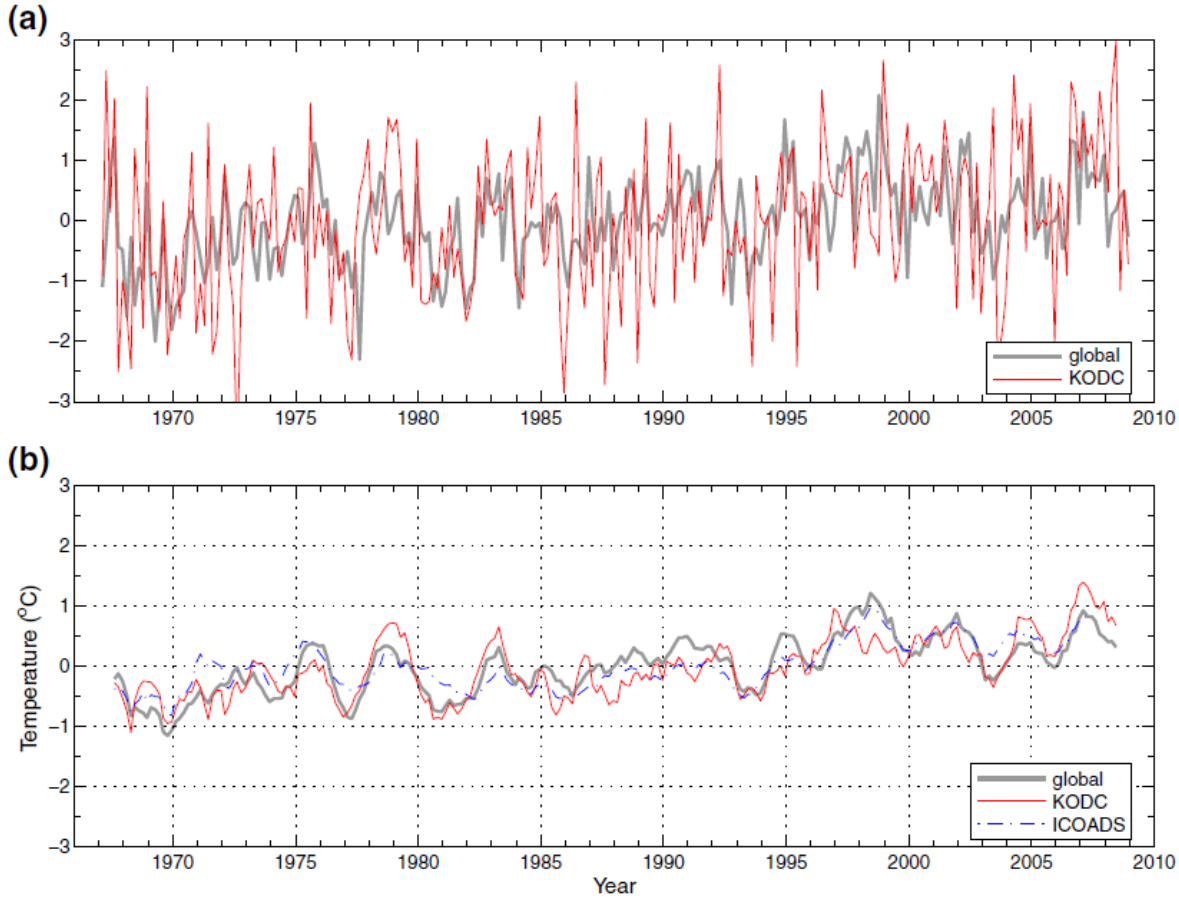

Fig. 3 SST anomaly time-series in the YSCWM from KODC (125°E, 35.9°N), global (124°E, 36.0°N; nearest to the KODC data location), and ICOADS: (a) before removing the seasonal cycle and (b) after removing the seasonal cycle. (*Park et al*, 2011)

The variability of YSCWM is usually represented by the temperature at bottom layers, such as 50m depth, to avoid the seasonal variation. The results in Park *et al* (2011) showed YSCWM revealed three cold events (1967–1971, 1983–1988 and 1996–2006) and two warm events (1972–1980 and 1990–1995), although the anomaly is little weak during 1990–1995. A relationship was also found between upper and bottom layers in summer: warm (cold) anomaly appears in the upper (bottom) layer in June/August during the cold (warm) events. In the cold events, as the

increased vertical temperature gradient of the thermocline impedes the downward heat transfer, the warming of YSCWM which peaks from June to August slows down in comparison with the normal years. In the warm events an opposite scenario occurs. Moreover, since the remnant of the winter Yellow Sea Warm Current Water remains in the Yellow Sea trough (Lie et al., 2001), YSCWM can be influenced by variability of the Yellow Sea Warm Current. Taking the Pacific Decadal Oscillation into account, the Yellow Sea Warm Current might be the last pathway that the Pacific Decadal Oscillation is transferred through the Kuroshio to the Yellow Sea.

2.2 Dissolved Oxygen (DO)

Based on the data from two co-operative cruises in 2008, the seasonal pattern of DO concentrations are shown in Fig. 4. In winter, DO concentrations decreased from west to east with levels above 9 mg/L in the west, and below 8 mg/L in the east. In the summer, the values of DO at surface (variation range of ca. 2mg/L) became lower toward the north central areas, whereas DO values at bottom (variation range of ca. 5mg/L) became lower toward the southern areas, and formed a hypoxia zone between 32^{o}N and 33^{o}N.

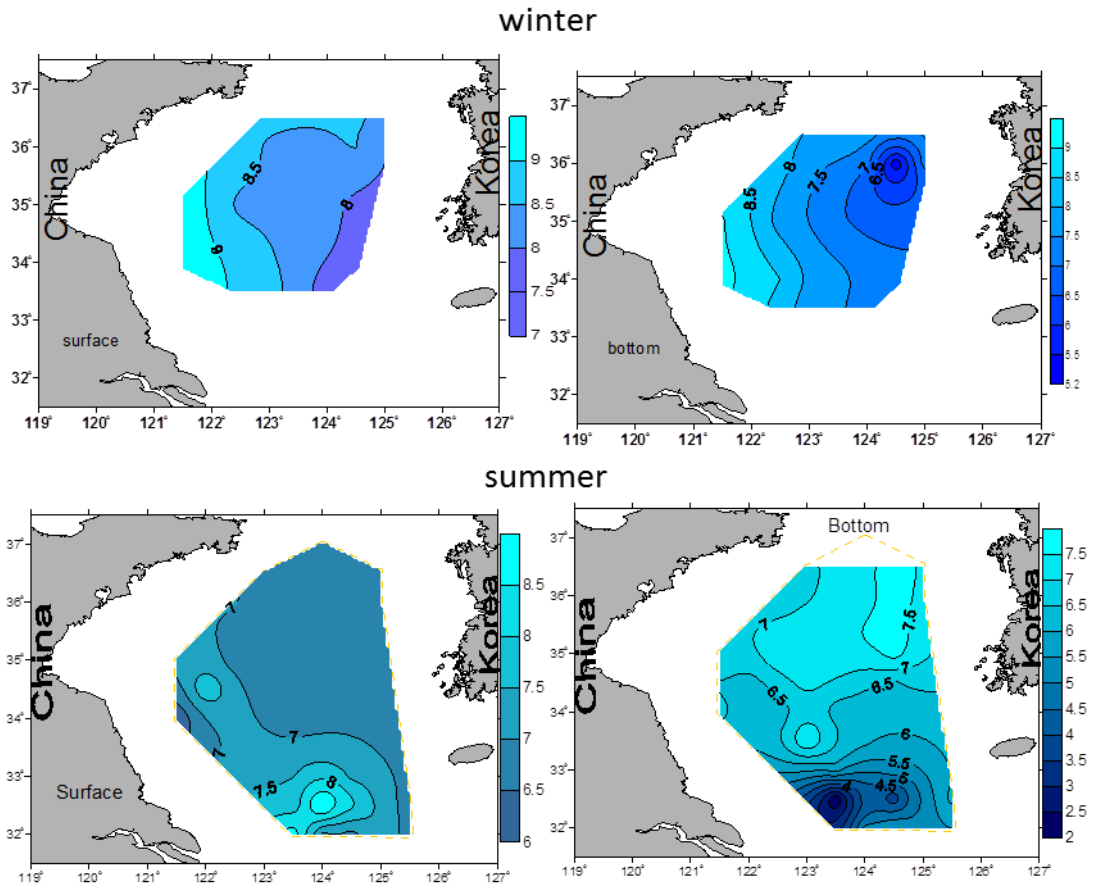

Fig.4 Seasonal comparison of DO concentrations in surface and bottom water layers in the YSCWM. Data are from two co-operative cruises in 2008 (UNDP/GEF cruises report, 2011).

The historical data from 1980s to 2012 showed that the horizontal distribution of DO had a general trend of higher concentrations in the northeast than those in the southwest (Fig. 5). A zone of high DO concentrations occurred in the northeastern region of the study area (122-123.5°E, 35-36°N), and the lowest DO concentrations were found in the southwest near the Changjiang plume. The annual mean DO concentration was relatively constant before 2008 and has maintained a lower level since. This observation was consistent with the horizontal DO distribution from the 1980s to 2012. The DO concentration on the Subei

shoalwas relatively lower (<8.5 mg L^{-1}) than that of other regions (>9 mg L^{-1}).

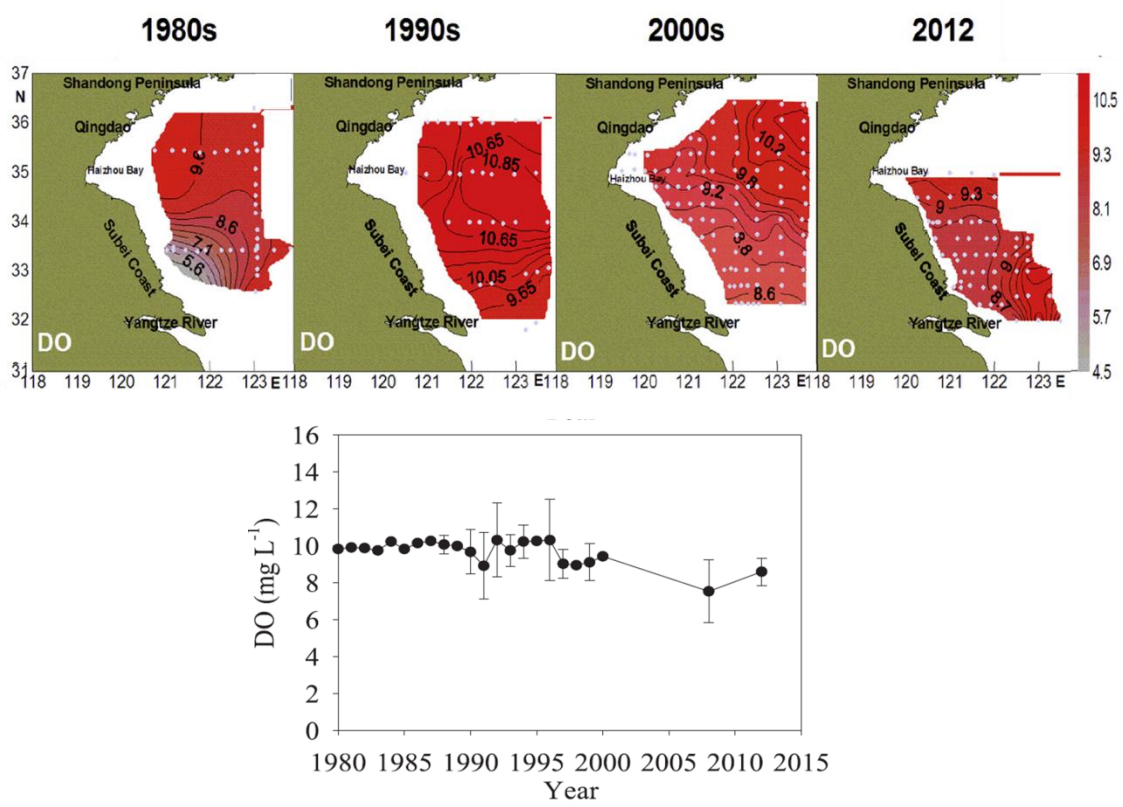

Fig.5 Inter-annual variability of surface DO concentrations in spring in South YS. Detailed sampling and data-analysis methods are described in Li et al (2015).

2.3 Dissolved Inorganic Nitrogen (DIN)

Based on the data from two co-operative cruises in 2008, the seasonal pattern of DIN concentrations are shown in Fig. 6. In winter, nitrate concentration varied in 5.19-12.42 μmol/L in the surface, and high levels were found in the northeast and decreased towards the southwest. Nitrite concentration ranged from 0.05-0.54 μmol/L, and high levels of nitrite were found in the northwest parts of the survey area, and decreased towards the southeast. Ammonia concentration varied in 0.48-2.33

μmol/L, and high levels of ammonia were found in the northwest side of the Yellow Sea and decreased gradually eastward. In summer, DIN was mostly depleted in the upper water column of YSCWM region.

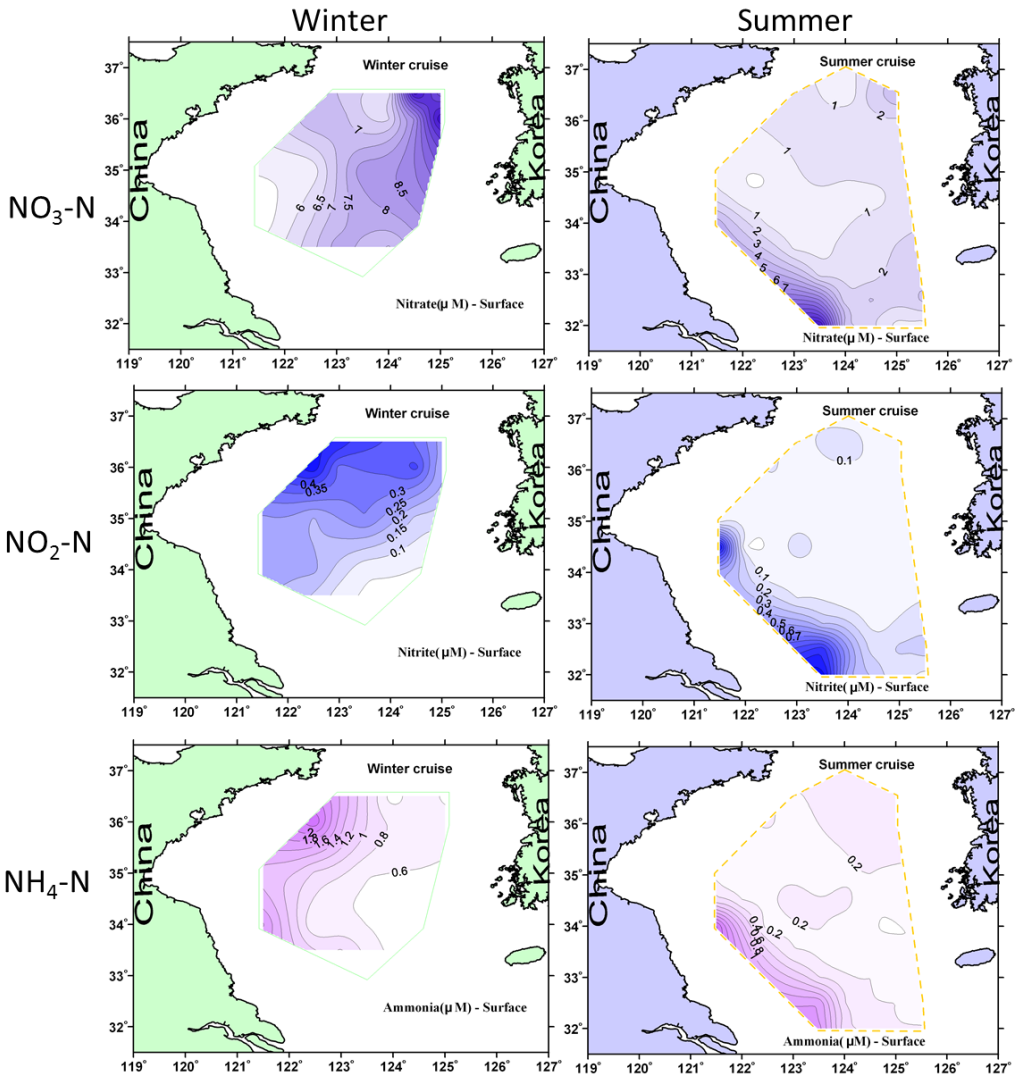

Fig.6 Seasonal comparison of nitrate, nitrite and ammonia concentrations in the surface water layers in the YSCWM. Data are from two co-operative cruises in 2008 (UNDP/GEF cruises report, 2011).

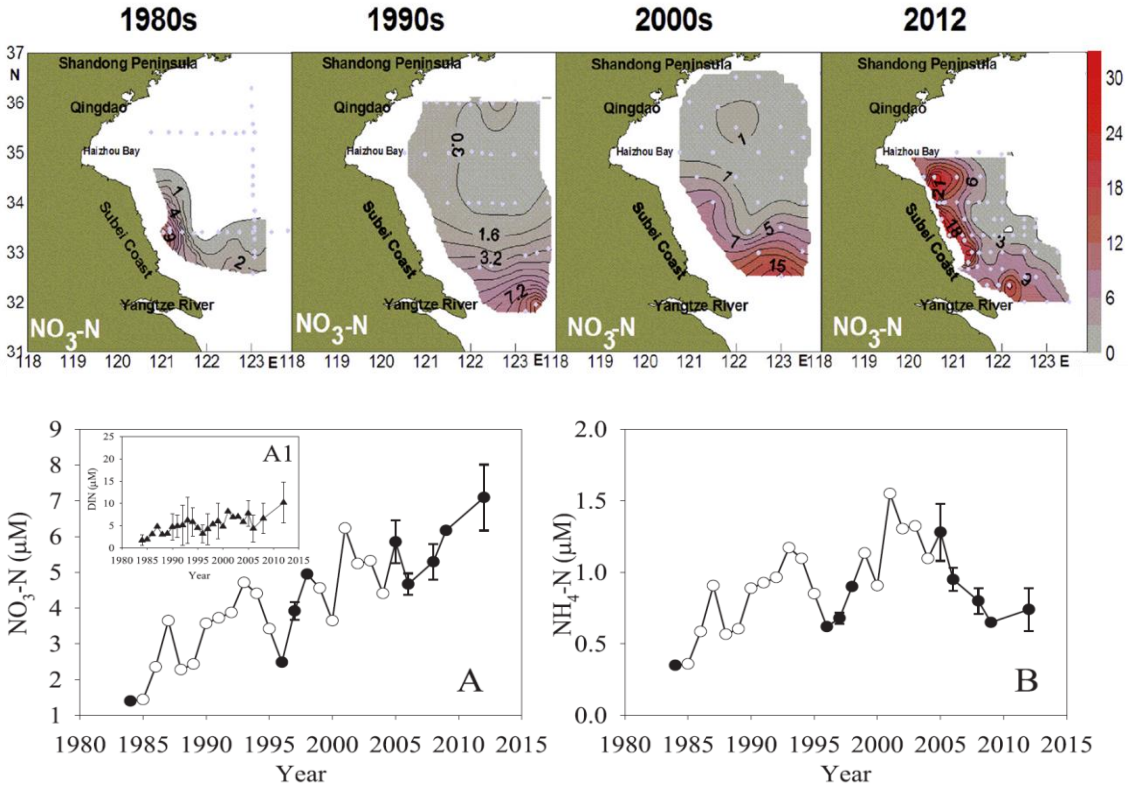

Fig.7 Inter-annual variability of surface nitrate and ammonia concentrations in spring in South YS. Detailed sampling and data-analysis methods are described in Li et al (2015).

The historical data from 1980s to 2012 showed a clear increasing trend in the horizontal distribution of NO_3-N from the 1980s to 2012 (Fig .7), with levels exceeding 23 μmol/L in the Subei shoal in 2012. The annual NO_3-N concentration also increased across the 30 years, and the level in 2012 was over 5× that in 1984. The substantial increase in NO_3-N values implied the significant nutrient contribution from the Yangtze plume into the SYS in recent years, thus the primary productivity would not be potentially limited by nitrogen in this area. By contrast, the annual NH_4-N value fluctuated during 1984-2012, and the level in 2012 was less 2× that in 1984, possibly indicating the role of nitrogen supply from biogeochemical

cycle in the SYS. It is a remarkable fact that the NO_3-N concentrations presented an increasing trend since 2006, while the NH4eN values descended simultaneously. This may be mainly attributable to the abundant terrestrial discharge in recent decade.

2.4 Phosphate

Based on the data from two co-operative cruises in 2008, the seasonal pattern of phosphate concentrations are shown in Fig. 8. In winter, phosphate concentrations varied between 0.33-1.66 μmol/L in the surface layer and 0.35-1.68 μmol/L in the bottom layer. Average phosphate concentrations were similar in different layers which were 0.73 μmol/L in the surface and 0.86 μmol/L in the bottom, respectively. The general spatal pattern of phosphate concentration in winter was higher in the southeast part and decreased westward. In summer, phosphate concentration varied between 0.01-0.1 3μmol/L in the surface layer and 0.10-1.14 μmol/L in the bottom layer. Mean concentrations in the surface were 0.05 μmol/L, which was much lower compared to winter. Due to thermal stratification, phosphate concentration at the bottom was significantly higher (averaged 0.62 μmol/L) than in the upper water column. High levels of phosphate were observed in the bottom layer of the YSCWM region.

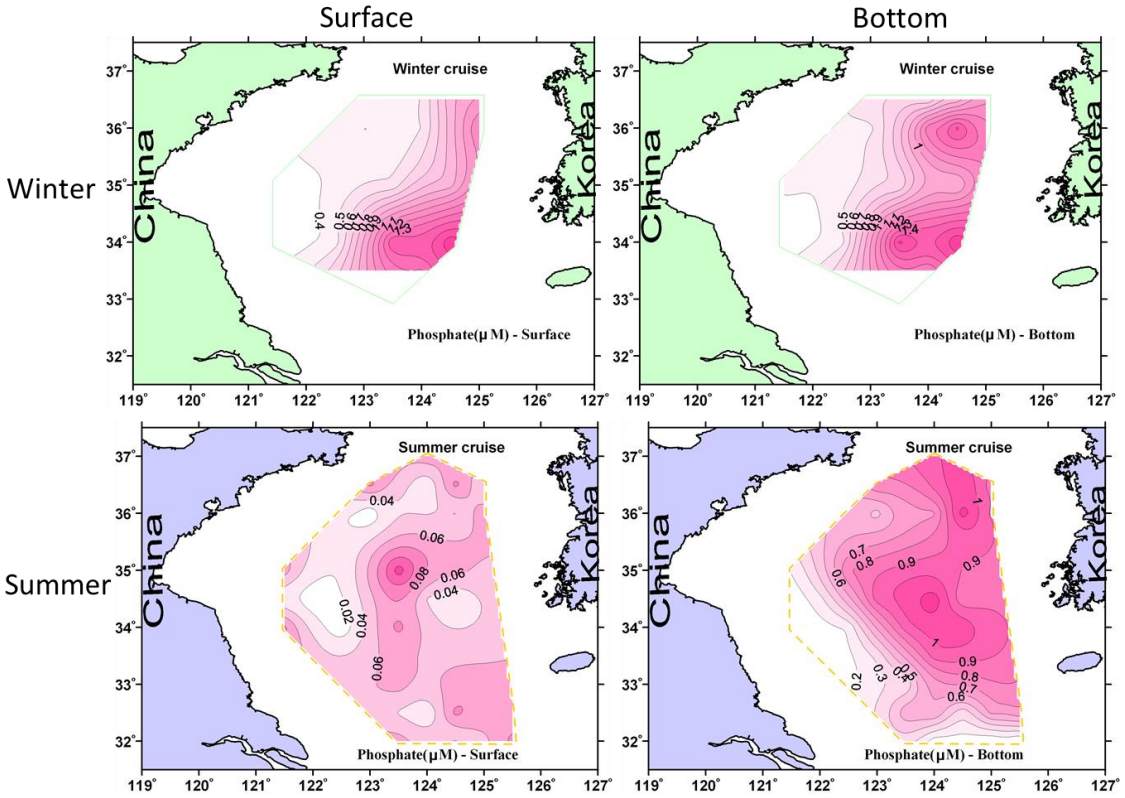

Fig.8 Seasonal comparison of phosphate concentrations in the surface and bottom water layers in the YSCWM. Data are from two co-operative cruises in 2008 (UNDP/GEF cruises report, 2011).

The historical data from 1980s to 2012 showed that the PO_4-P concentration was highest in the 1980s and then decreased in 1997, but was again elevated and the high concentration zone expanded in 2006, and eventually decreased again in 2012 (Fig. 9). The annual PO_4-P concentration also fluctuated from the 1980s to 2005 and has since decreased. This trend occurred because PO_4-P concentrations were affected not only by terrestrial discharge, but also by phytoplankton uptake and ocean water input.

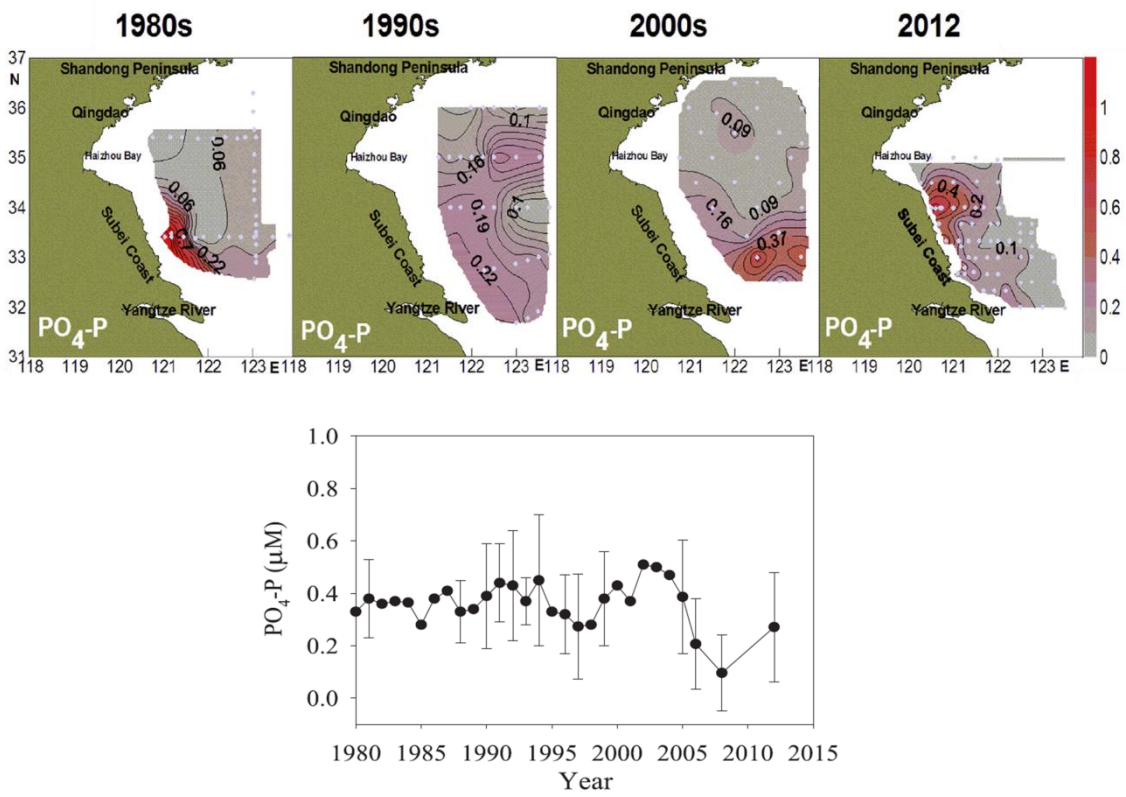

Fig.9 Inter-annual variability of surface phosphate concentrations in spring in South YS. Detailed sampling and data-analysis methods are described in Li et al (2015).

2.5 Silicate

Based on the data from two co-operative cruises in 2008, the seasonal pattern of silicate concentrations are shown in Fig. 10. In winter, silicate concentration varied between 6.89-14.07 μmol/L in the surface layer and 7.63-17.82 μmol/L in the bottom layer. Average silicate concentrations in the bottom layer (11.17 μmol/L) were higher compared with that in surface (9.57 μmol/L). The distribution feature of silicate in winter was similar to that of nitrate, with high levels in the central and northeast parts.

In summer, silicate concentrations varied between 0.01-8.16 μmol/L in the surface layer and 3.21-27.84 μmol/L in the bottom layer. Average concentration increased with depth and changed from 2.78 μmol/L in the surface to 13.46 μmol/L in the bottom. Similar to nitrate and phosphate, mean values of silicate at the bottom were significantly higher than in the upper water column. High levels of silicate were observed in the bottom layer of the YSCWM region.

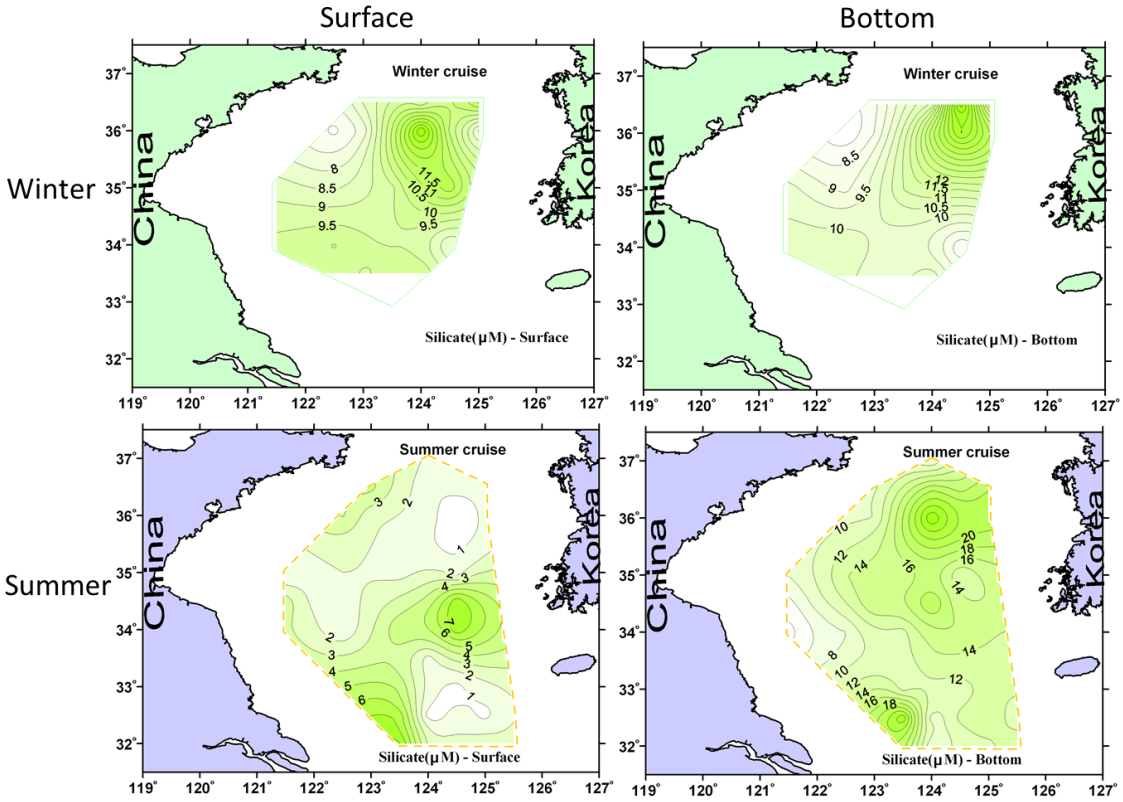

Fig. 10 Seasonal comparison of silicate concentrations in the surface and bottom water layers in the YSCWM. Data are from two co-operative cruises in 2008 (UNDP/GEF cruises report, 2011).

The historical data from 1980s to 2012 showed that silicate concentrations were lower in the 1980s, and then appeared a slightly fluctuating trend in the years since (Fig. 11). Annual mean SiO_3-Si concentrations also

fluctuated during these decades. Concentrations declined slightly (by 8.6%) over the entire time period (i.e., between 1980 and 2012), which indicated that SiO_3-Si was possibly not a crucial factor for green tide bloom in the SYS.

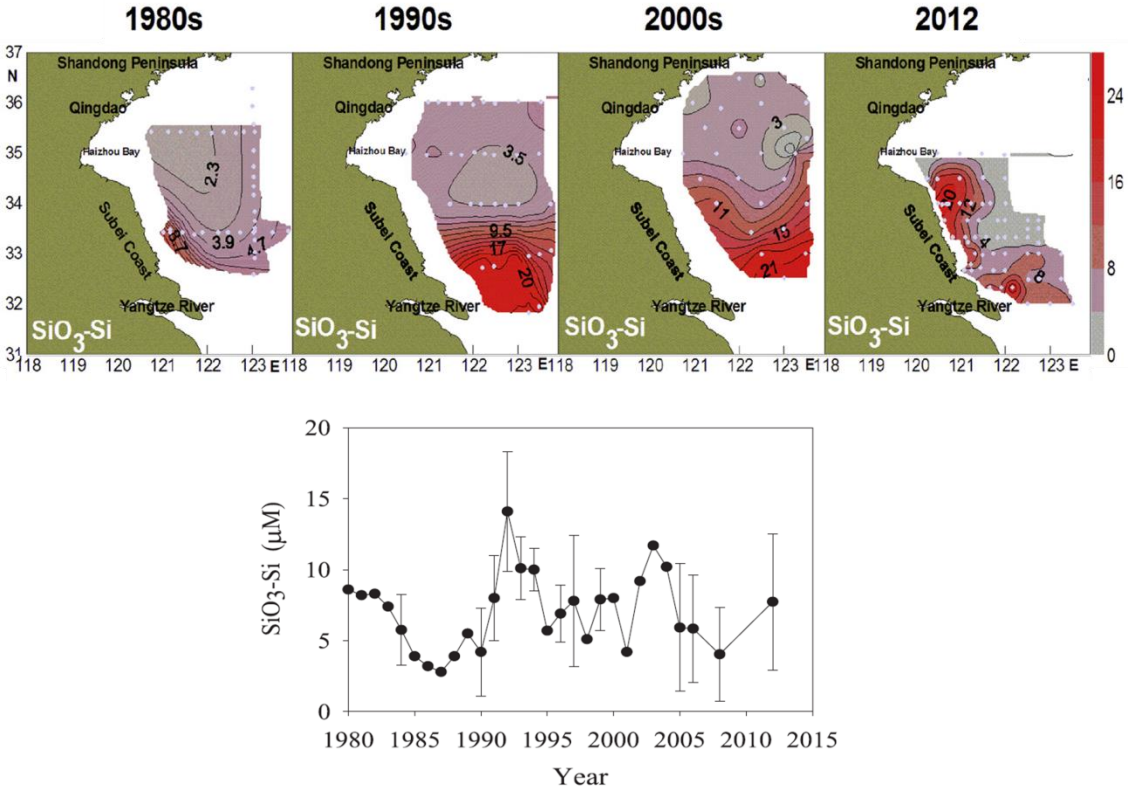

Fig.11 Inter-annual variability of surface silicate concentrations in spring in South YS. Detailed sampling and data-analysis methods are described in Li et al (2015).

3. Structure of plankton communities in the YSCWM region

Net samples data from two co-operative cruises in the YSLME were used here to show the characteristics of plankton communities in the Yellow Sea. These two cruises were carried out in the Southern Yellow Sea in 2008, one in winter (17 to 31 January) and another in summer (2 to 13 August). Detailed sampling methods have been described in the UNDP/GEF cruises report (2011).

3.1 Phytoplankton

Table 1. Dominant species of net phytoplankton samples in 2008. Dominance (Y) was calculated by the product of proportional abundance of the specific species (n_i/N) and its occurrence frequency (f_i).

Winter		Summer	
Species	Dominance	Species	Dominance
Corethron hystrix	0.051	*Chaetoceros lorenzianus*	0.239
Chaetoceros densus	0.039	*Chaetoceros* spp.	0.039
Ditylum brightwelli	0.032	*Chaetoceros affinis*	0.030
Chaetoceros lorenzianus	0.029	*Chaetoceros pseudocurvisetus*	0.013
Coscinodiscus oculus-iridis	0.028	*Pseudonitzschia pungens*	0.010
Odontella sinensis	0.028		
Bacillaria pacillifera	0.025		
Coscinodiscus wailesii	0.016		
Ceratium intermedium	0.015		
Coscinodiscus sp.	0.015		
Pseudonitzschia pungens	0.013		
Guinardia flaccida	0.013		
Coscinodiscus asteromphalus	0.010		

There were a total of 62 and 139 species of phytoplankton identified in

winter and summer, respectively. In winter, the number of dominant species is much more than that in summer (Table 1). *Chaetoceros lorenzianus* and *Pseudonitzschia pungens* are the common dominant species in both seasons.

In the net samples collected in winter, several diatoms dominated with similar dominance indexes. For example, the abundance of *Corethron hystrix* was higher in the north than that in the south, while *Chaetoceros densus* showed high density in the central zone and was not found in the southeast part of the study area (Fig. 12).

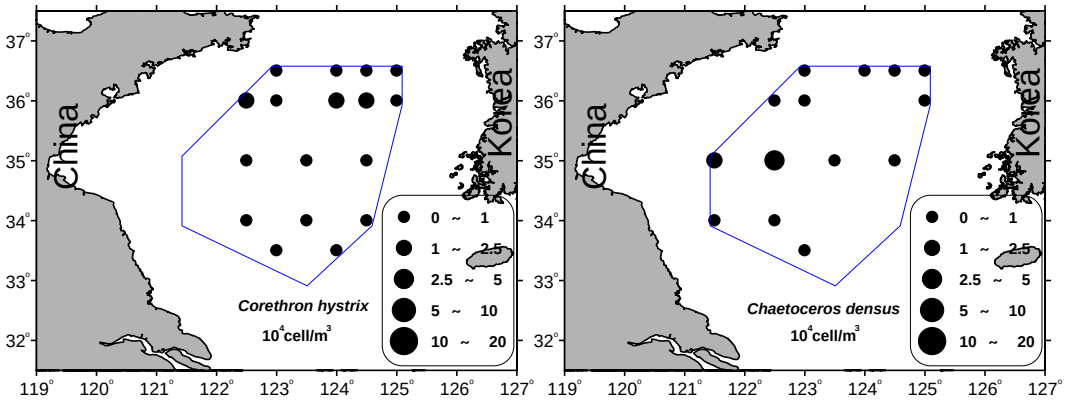

Fig. 12. Distribution of *Corethron hystrix* (left) and *Chaetoceros densus* (right) in net samples in winter.

In the summer net samples, the genus *Chaetoceros* was the most dominant taxon with an average of 632×10^4 cells/m^3, and accounted for 87.8% of total abundance. It defined the horizontal distribution features of phytoplankton abundance, i.e., the overall distribution pattern showed higher values in the southwest and low values in most other parts (Fig. 13).

Chaet. lorenzianus was the most dominant species, averaging 374×10^4 cells/m^3, and accounting for 52% of the total abundance. This species shaped the main features of total abundance in the net samples.

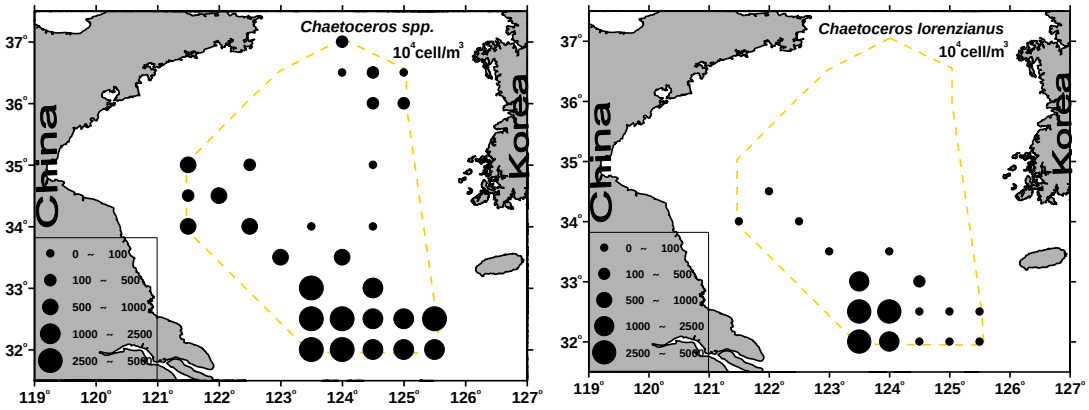

Fig. 13. Distribution of *Chaetoceros spp.* (left) and *C. lorenzianus* (right) in the summer net samples.

Net sampled phytoplankton species diversity (*H'*) in winter varied between 0.22-4.24. The highest diversity occurred at the stations with high cell abundance (southwest zone). In general, the species diversity indexes of phytoplankton were higher in the south as compared to the north (Fig. 14, left panel). In the summer, the diversity of net samples scored from 0.19-3.84 with a mean value of 1.87. Low levels of diversity were found in the southeast and northwest (Fig. 14, right panel).

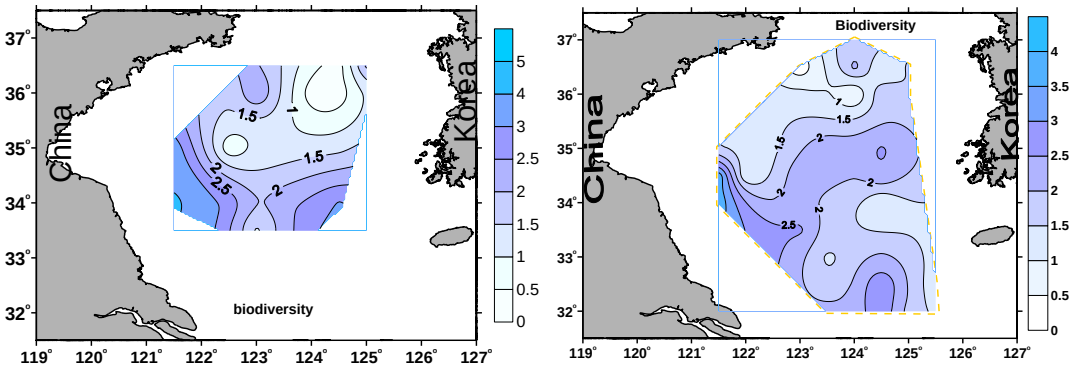

Fig. 14. Species diversity (*H'*) of phytoplankton community in winter (left) and summer (right).

3.2 Zooplankton

Data from the samples collected with the 505 μm mesh plankton net were used here to show the zooplankton community structure. In winter, a total of 71 zooplankton species (otherwise lowest taxonomy level) were identified, including copepods (26 species), larvae (18 species), mysidacea (6 species), medusa (5 species), mastigopus (3 species), chaetognaths (2 species), euphausiids (2 species), and other groups. In summer, a total of 77 zooplankton species were identified, including copepods (37 species), medusa (11 species), mysids (9 species), tunicates (4 species), pteropods (3 species), decapods (3 species), and other groups. The survey results showed that *Calanus sinicus* and *Sagitta crassa* were the main dominant species in the YSCWM area, and the composition of dominant species was similar between winter and summer (Table 2).

Table 2. Dominant species of net zooplankton samples in 2008. Dominance (Y) was calculated by the product of proportional abundance of the specific species (n_i/N) and its occurrence frequency (f_i).

Winter		Summer	
Species	Dominance	Species	Dominance
Sagitta crassa	0.383	*Calanus sinicus***	0.467
Calanus sinicus	0.343	*Sagitta crassa***	0.175
Oithona plumifera	0.092	*Oithona plumifera**	0.054
Parathemisto gaudichardi	0.036	*Parathemisto gaudichardi*	0.048
		Macrura larvae	0.020

In winter, *Sagitta crassa* was the most abundant species, and its abundance varied between 4 and 202 ind./m^3 (mean: 98 ind./m^3). There was higher abundance of *S. crassa* in the western coastal areas than that in the open sea (Fig. 15, left panel). The abundance of *Calanus sinicus* varied between 2 and 205 ind./m^3 (mean: 37 ind/m^3). There was higher abundance of *C. sinicus* in the north than that in the middle and south (Fig. 15, right panel).

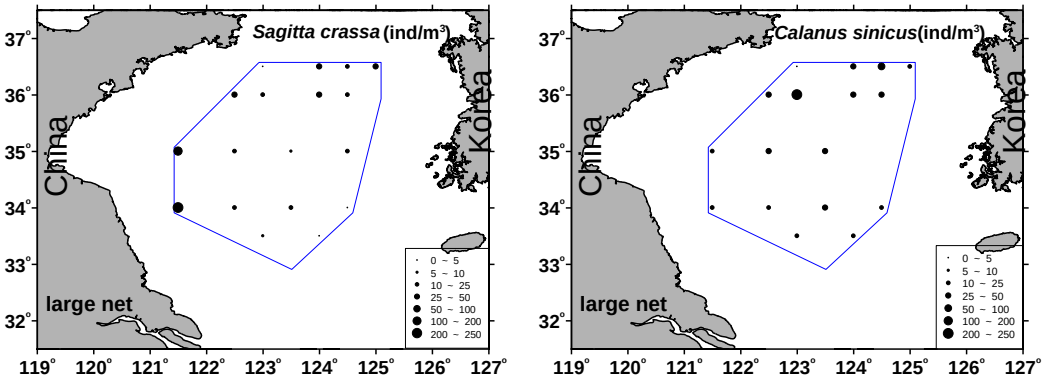

Fig. 15. Distribution of *Sagitta crassa* (left) and *Calanus sinicus* (right) abundance in winter.

In summer, *C. sinicus* was the most abundant species and largely contributed to total individual density. The abundance of *C. sinicus* varied

from 1 to 536 ind./m^3 and the magnitude was much higher (mean: 113 ind./m^3) than that in winter (mean: 37 ind./m^3). *C. sinicus* was evenly distributed throughout most of the study area (Fig. 16, left panel). The abundance of *S. crassa* varied from 2 to 202 ind./m^3 (mean: 40 ind./m^3), and the most abundant zone was located at the west and north of the study region (Fig. 16, right panel).

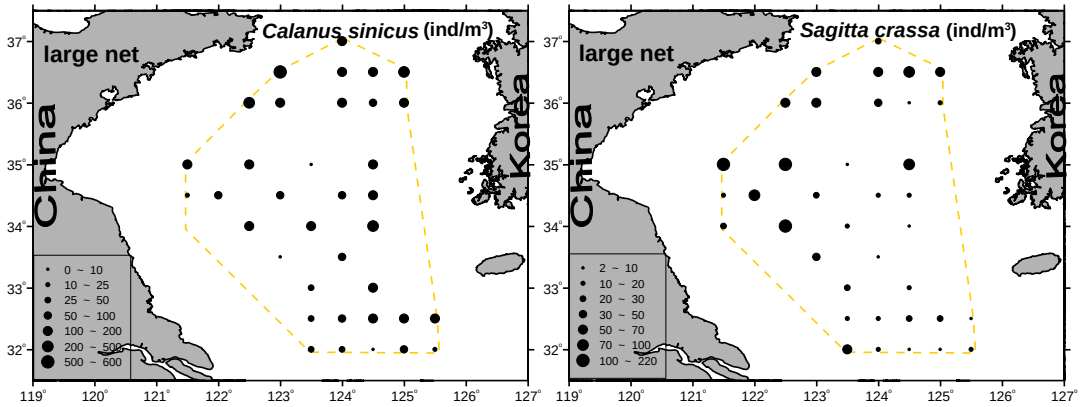

Fig. 16. Distribution of *Calanus sinicus* (left) and *Sagitta crassa* (right) abundance in summer.

The non-gelatinous zooplankton biomass in winter averaged 110.5 mg/m^3 (in the range of 17.5-285.4 mg/m^3) in the south YSCWM area, and lower biomass was found in the central and northern zones (Fig. 17, left panel). In summer, zooplankton biomass averaged 194.0 mg/m^3 (in the range of 13.2-606.2 mg/m^3), and higher biomass was found in the southeast zone (Fig. 17, right panel).

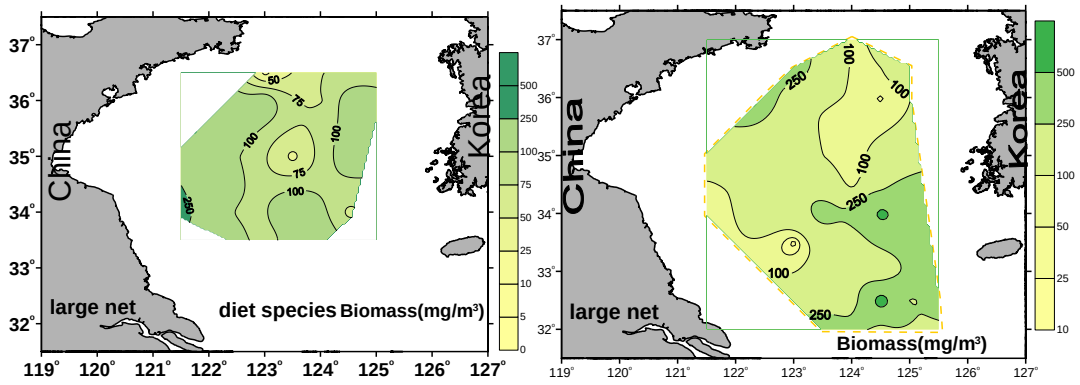

Fig. 17. Distribution of zooplankton biomass (mg/m^3) in winter (left) and summer (right).

In winter, the diversity index of zooplankton community was in the range of 0.64-2.87, and the lowest biodiversity was found in the west coastal areas and increasing from northwest to the southeast (Fig. 18, left panel). In summer, the diversity index was in the range of 0.92-3.16, and the higher biodiversity was found in the southern areas and decreasing from southwest to northeast (Fig. 18, right panel).

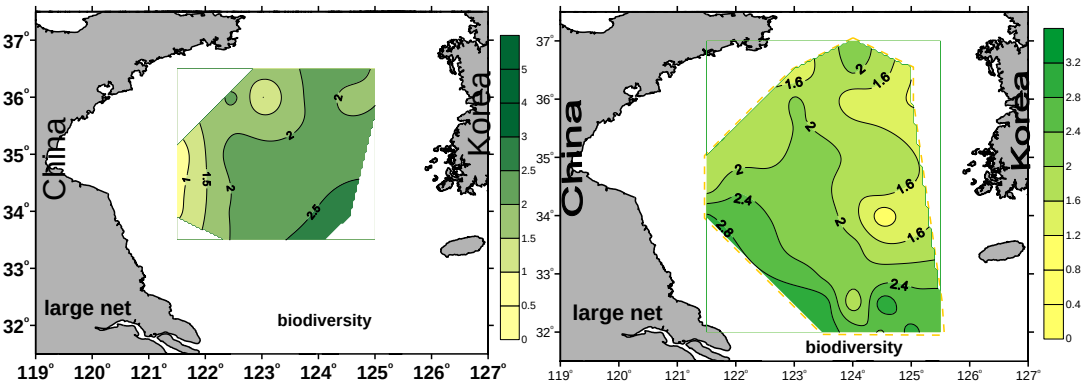

Fig. 18. Species diversity (*H'*) of zooplankton community in winter (left) and summer (right).

4. Relationships between environment change and plankton community in the YSCWM region

To our knowledge, up to now, there are relatively few long time-series of plankton abundance and distribution available in the YSCWM region to quantitatively assess the relationship between environment change and plankton community. The factors influencing plankton community in the YSCWM region are very difficult to be identified from so complex system, including many physical-chemical- biological interactions. From the trophic relationships in the marine food chains, the phytoplankton are mainly influenced by light, temperature, nutrients and herbivorous grazers in the ocean, while the zooplankton are mainly influenced by phytoplankton and nekton, through bottom-up effect of food supply and top-down control of predators.

For the temporal variation of phytoplankton, the average Chl-a concentration in the surface water of the southern Yellow Sea varied between 0.11 mg/m^3 and 1.62 mg/m^3 during 1983-2008. The Chl-a concentrations were lower in 1996–1998 as compared to 1983–1986, followed by the suggestion of an increasing trend through at least 2007, with the highest values of the record during 2006–2007, all higher than 1 mg/m^3 (Fig. 19). Phytoplankton cell abundance (net samples) has shown

great fluctuations in the past 50 years, spanning at least 4 orders of magnitudes over the record (Fig. 19). The highest abundance was recorded during summer 2006 (63363×10^4 cell m^{-3}) whereas the lowest value was only 2.59×10^4 cell m^{-3}, recorded during May 2005. At present, no clear trend can be discerned in the historic dataset.

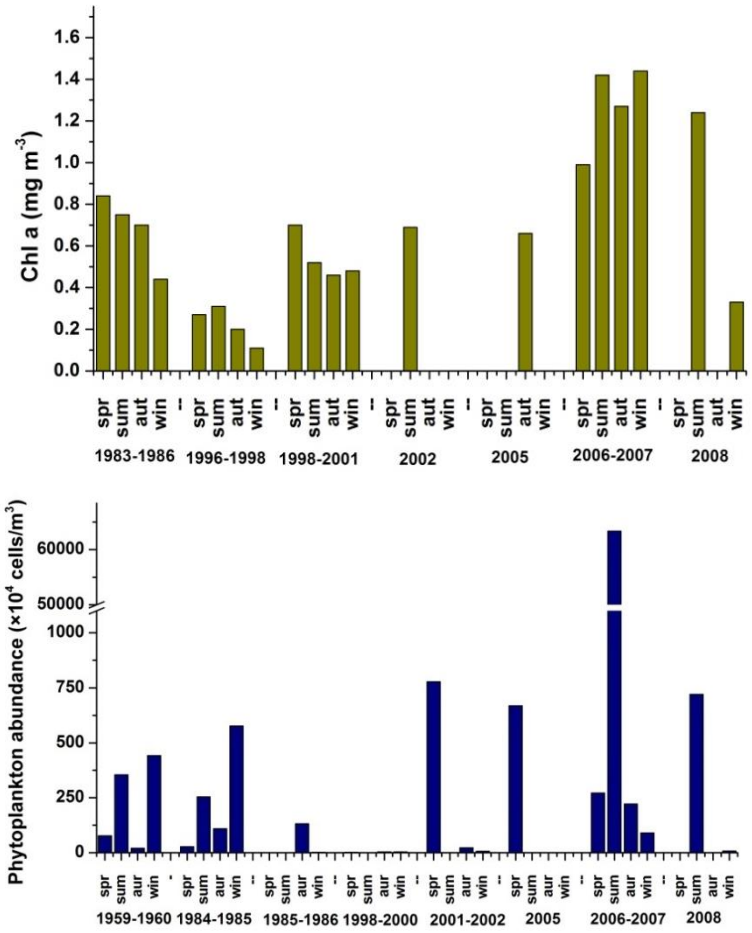

Fig. 19. Long term variability of chlorophyll *a* concentrations and phytoplankton abundance in southern Yellow Sea (Fu *et al*, 2012)

Although the effects of temperature on diatom cell size and growth rates have been validated in laboratory cultured phytoplankton species

(Montagnes and Franklin, 2001), field results did not seem to support any obvious relationship between phytoplankton biomass and temperature (Fu et al., 2009). In the natural environment of ocean, temperature and nutrient are strongly covariant (Agawin et al., 2000), the effects of temperature is more important by changing the nutrient availability rather than its direct influence on the growth of phytoplankton.

For the temporal variation of zooplankton, Liu et al (2012) suggested the seasonal pattern of the zooplankton biomass was spring and summer higher than autumn and winter in 2006-2007, which is consistent with that in 1958-1959 and 2000-2001 (Fig. 20). Among the long term comparison of the mean zooplankton biomass, 2006-2007 is highest, 2000-2001 comes second, 1958-1959 and 1984-1985 are relatively lowest. The zooplankton biomass has an increasing trend in recent years from the long term variability shown in Fig. 20. Additionally, the contribution of gelatinous zooplankton to total zooplankton biomass is much more than that of non-gelatinous zooplankton, which agrees with the frequent macro-jellyfish blooms in the Yellow Sea since the middle and later in the 1990s and even resulting in an ecological disaster in recent years.

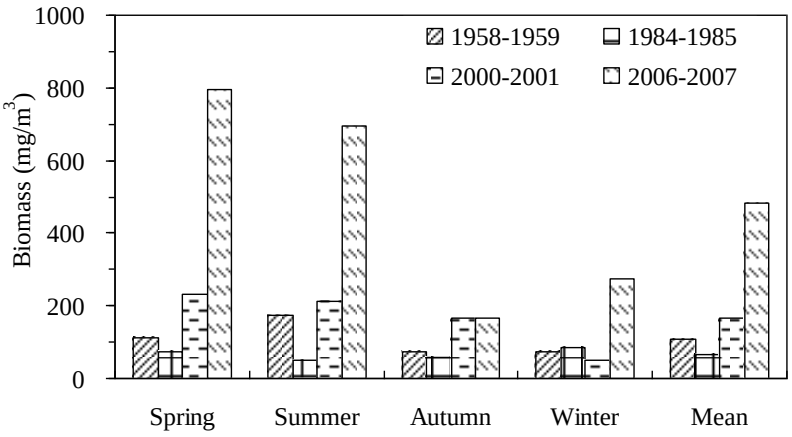

Fig. 20. Long term variability of the total zooplankton biomass in the southern Yellow Sea (Liu *et al*, 2012)

The inter-annually seasonal variations in abundance of *C. sinicus* showed a significant difference between different years in the northern YSCWM (Fig. 21). The abundance of *C. sinicus* was significantly higher in 2011–2014 than that in 1959 and 1982. The overall mean abundance was 182.5 ind./m^3 in 2011–2014, which was 5.5 times than that in 1959. The abundance of *C. sinicus* in 2006–2007 was also significantly higher than that in 1959 and 1982. The overall mean abundance in 2006–2007 was 191.8 ind./m^3, which was 5.7 times as much as that in 1959. Further analysis shows a greater increase of its abundance in the northern YS than the southern YS and the northern ECS, suggesting a different response patterns to climate variability when compared with the subtropical seas along the Chinese coast (Yang et al, 2018).

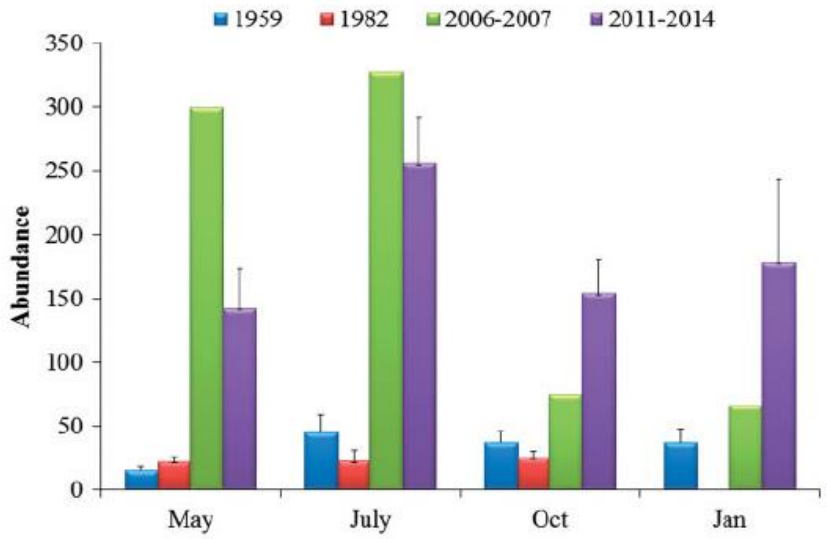

Fig. 21. Long term variability of *Calanus sinicus* abundance in the northern YS (Yang *et al*, 2018)

Our latest study on the phenology of seasonal phytoplankton blooms in the Yellow Sea showed also a certain relationship between temperature changes and phytoplankton dynamics. Seasonal warming and cooling may not only affect phytoplankton physiological processes but also change the stratified conditions in ways that exert controls on bloom dynamics. Relatively fast surface warming causes an earlier and stronger spring bloom in the South Yellow Sea. Meanwhile, fast cooling might be responsible for the weak autumn blooms in the specific zones. Shoaling stratification driven by fast warming can maintain the rapid growth of phytoplankton due to the light and nutrient advantages in surface waters. A similar explanation is applicable for the impact of slow warming on the weak spring bloom. For different seasonal blooms, the bottom-up responses may vary spatially. For example, under future climate scenarios,

seasonal warming/cooling rates in spring/autumn could be intensified in the YS. This could promote the development of an earlier spring bloom and further weaken autumn bloom in the central area, and potentially enhance the growth rate and thus the magnitude of the winter bloom in the warmer coastal water. However, in the summer-bloom region, changes in the seasonal warming/cooling rate likely play a less important role than river run-off variability. (Song et al, 2019).

5. Conclusion

While the impact of climate on the physical processes in the Yellow Sea has received much attention, more efforts are needed to better understand the biological responses. Sea surface temperature changes in the YSCWM region can be easily obtained from transect observations and satellite-derived data. However, structure of plankton communities should be based on the analysis of taxonomy data from plankton samples. In this region, there are no enough cruise data to support this topic, especially in the long term effect of climate change. Moreover, there are large errors of plankton taxonomy data among different sources, and it will exceed the changes driven by climate. Therefore, it is difficult to give a quantitative analysis on this topic. The interannual variability of plankton community and their relationships to physical forcings are less clear and warrant further investigation.

Future studies will require long-term and intensive in situ observations at multiple sites in this spatially heterogeneous system. Moreover, high-resolution biological-physical modeling focusing on plankton dynamics is highly recommended to clearly understand the underlying mechanisms in this dynamically complex and socioeconomically important ecosystem.

References

1) Agawin N R S, Duarte C M, Agustı S, 2000. Nutrient and temperature control of the contribution of picoplankton to phytoplankton biomass and production. Limnology and Oceanography 45, 591–600.

2) Fu M Z, Wang Z L, Pu X M *et al*, 2012. Changes of nutrient concentrations and N:P:Si ratios and their possible impacts on the Huanghai Sea ecosystem. Acta Oceanologica Sinica, 31 (4): 101–112

3) Fu M, Wang Z, Li Y, *et al*., 2009. Phytoplankton biomass size structure and its regulation in the Southern Yellow Sea (China): Seasonal variability. Continental Shelf Research, 29: 2178-2194.

4) Li H M, Zhang C S, Han X R, *et al*., 2015. Changes in concentrations of oxygen, dissolved nitrogen, phosphate, and silicate in the southern Yellow Sea, 1980-2012: Sources and seaward gradients. Estuarine, Coastal and Shelf Science, 163: 44-55.

5) Lie H J, Cho C H, Lee J H, *et al*, 2001. Does the Yellow Sea Warm Current really exist as a persistent mean flow? J. Geophys. Res. 106 (C10), 22199–22210.

6) Lin C L, Ning X R, Su J L *et a1*, 2005. Enviromental changes and respondes of ecosystem of the Yellow Sea during 1976—2000. Journal of Marine Systems, 55: 223–234

7) Liu P, Song H, Wang X, *et a1*, 2012. Seasonal variability of the zooplankton community in the southwest of Huanghai Sea (Yellow Sea) Cold Water Mass. Acta Oceanologica Sinica, 31(4):127-139.

8) Montagnes D J, Franklin D J, 2001. Effect of temperature on diatom volume, growth rate, and carbon and nitrogen conten: reconsidering some paradigms. Limnology and Oceanography 46, 2008–2018.

9) Park S, Chu P C, Lee J. 2011. Interannual-to-interdecadal variability of the Yellow Sea Cold Water Mass in 1967-2008: Characteristics and seasonal forcings. Journal of Marine Systems, 87(3-4):177-193.

10) Park S, Chu P C. 2006. Thermal and haline fronts in the Yellow/East China Seas: surface and subsurface seasonality comparison. Journal of Oceanography, 62 (5), 617–638.

11) Song H, Ji R, Xin M, et al. 2019. Spatial heterogeneity of seasonal phytoplankton blooms in a marginal sea: physical drivers and biological responses. ICES Journal of Marine Science, doi:10.1093/icesjms/fsz176.

12) UNDP/GEF. 2011. Seasonal variation of the major environmental parameters in the Yellow Sea Basin. UNDP/GEF Yellow Sea Project, Ansan, Republic of Korea (102 pages).

13) Wang R, Zuo T, Wang KE. 2003. The Yellow Sea Cold Bottom Water—an oversummering site for *Calanus sinicus* (Copepoda, Crustacea). Journal

of Plankton Research, 25(2): 169-183.

14) Yang Q, Liu H, Liu G, Gu Y. 2018. Spatio-temporal distribution pattern of *Calanus sinicus* and its relationship with climate variability in the northern Yellow Sea. ICES Journal of Marine Science, 75(2): 764-772.